UNIVERSITY OF COPENHAGEN

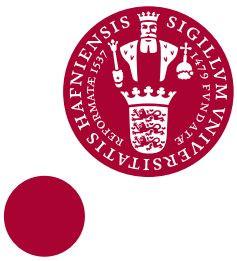

# R(K-(*)) from dark matter exchange

Cline, James M.; Cornell, Jonathan M.

*Published in:*
Physics Letters B

*DOI:*
10.1016/j.physletb.2018.05.034

*Publication date:*
2018

*Document version*
Publisher's PDF, also known as Version of record

*Document license:*
CC BY

*Citation for published version (APA):*
Cline, J. M., & Cornell, J. M. (2018). R(K-(*)) from dark matter exchange. *Physics Letters B*, *782*, 232-237. https://doi.org/10.1016/j.physletb.2018.05.034

Download date: 05. maj. 2023

Physics Letters B 782 (2018) 232–237

Contents lists available at ScienceDirect

Physics Letters B

www.elsevier.com/locate/physletb

# $R(K^{(*)})$ from dark matter exchange

James M. Cline [a,b,*], Jonathan M. Cornell [b]

[a] Niels Bohr International Academy & Discovery Center, Niels Bohr Institute, University of Copenhagen, Blegdamsvej 17, DK-2100, Copenhagen, Denmark
[b] McGill University, Department of Physics, 3600 University St., Montréal, QC H3A2T8, Canada

ARTICLE INFO

*Article history:*
Received 26 February 2018
Received in revised form 19 April 2018
Accepted 11 May 2018
Available online 15 May 2018
Editor: B. Grinstein

ABSTRACT

Hints of lepton flavor violation have been observed by LHCb in the rate of the decay $B \to K\mu^+\mu^-$ relative to that of $B \to Ke^+e^-$. This can be explained by new scalars and fermions which couple to standard model particles and contribute to these processes at loop level. We explore a simple model of this kind, in which one of the new fermions is a dark matter candidate, while the other is a heavy vector-like quark and the scalar is an inert Higgs doublet. We explore the constraints on this model from flavor observables, dark matter direct detection, and LHC run II searches, and find that, while currently viable, this scenario will be directly tested by future experiments.

© 2018 The Author(s). Published by Elsevier B.V. This is an open access article under the CC BY license (http://creativecommons.org/licenses/by/4.0/). Funded by SCOAP[3].

## 1. Introduction

The LHCb experiment has observed intriguing deficits in $R(K)$ and $R(K^*)$, defined as the ratio of branching ratios $B(K^{(*)} \to \mu^+\mu^-)/B(K^{(*)} \to e^+e^-)$ [1,2]. These "hadronically clean" ratios are free from theoretical uncertainties in hadronic matrix elements, which cancel out [3]. In the standard model (SM) it is expected that $R(K^{(*)}) = 1$ [4], while experimentally deficits of approximately 20% are observed. Although the significance in either observation $K$ or $K^{(*)}$ is not high, model-independent fits to both data, and possibly including quantities more sensitive to hadronic physics, including $B_s \to \mu^+\mu^-$, $B_s \to \phi\mu^+\mu^-$ and the angular observable $P_5'$, indicate a higher significance of $\sim 4\sigma$ [5–9]. Ref. [10] shows that the best fits and significance do not change appreciably whether one includes the hadronically sensitive observables or not, and that it is possible to find a good fit to the data by including a single dimension-6 operator in the effective Hamiltonian,

$$H_{\rm eff} \ni \mathcal{O}_{b_L\mu_L} = \frac{1}{\Lambda^2}(\bar{s}_L\gamma_\alpha b_L)(\bar{\mu}_L\gamma^\alpha\mu_L) \qquad (1)$$

with $\Lambda \cong 31$ TeV, which is approximately $-0.15$ times the SM contribution at one loop.

The new physics contribution (1) can be obtained from tree-level exchange of a heavy $Z'$ vector boson [11–18] or leptoquark [19–36], or through loop effects of new particles. In ref. [37], an exhaustive classification and study of the simplest loop models was carried out, where it was shown that one needs either two new scalars and one new fermion, or two new fermions and one new scalar, to explain the $B$ decay anomalies. Many possible quantum numbers of the new particles are possible. Here we note that these include cases where one of them can be neutral under the SM gauge interactions, opening the possibility that it could be dark matter (DM), and thus allowing the model to explain two observed phenomena requiring new physics.

We prefer to minimize the number of new scalars so there is just one, thereby allowing the DM candidate to be one of the new fermions.[1] Fermionic dark matter is free from relevant Higgs portal couplings, making for a more predictive theory in which the dark matter properties are determined by the same couplings that explain the flavor anomaly. It will be shown that considerations of the dark matter relic density and direct detection give interesting additional restrictions on the model, and that it is also constrained by existing LHC searches as well as flavor-changing neutral current

* Corresponding author.
*E-mail addresses:* jcline@physics.mcgill.ca (J.M. Cline), cornellj@physics.mcgill.ca (J.M. Cornell).

[1] Ref. [38] focuses on the opposite choice, and observes that the possible scalar dark matter candidate cannot satisfy direct detection constraints because of its coupling to $Z$. Previous attempts to connect $R(K^{(*)})$ to dark matter can be found in refs. [39–46]. In addition, refs. [47,48] recently studied models similar to ours, but in which the DM is chosen to be a new scalar. These studies do not fully consider the impact of the Higgs portal coupling $\lambda|H|^2|\phi|^2$ on the DM relic density and direct detection. In ref. [49] it was shown that $\lambda$ tends to dominate over any other new physics effects. Even if it vanishes at tree level, the one-loop correction tends to be too large to ignore without fine tuning.

https://doi.org/10.1016/j.physletb.2018.05.034
0370-2693/© 2018 The Author(s). Published by Elsevier B.V. This is an open access article under the CC BY license (http://creativecommons.org/licenses/by/4.0/). Funded by SCOAP[3].

**Table 1**
Quantum numbers of new physics particles, including accidental $Z_2$ discrete symmetry that insures stability of the dark matter $S$, baryon ($B$) and lepton ($L$) number. SM particles do not transform under the $Z_2$.

| | SU(3) | $SU(2)_L$ | $U(1)_y$ | $U(1)_{em}$ | $Z_2$ | $L$ | $B$ |
|---|---|---|---|---|---|---|---|
| $\Psi$ | 3 | 1 | +2/3 | +2/3 | −1 | −1 | +1/3 |
| $S$ | 1 | 1 | 0 | 0 | −1 | 0 | 0 |
| $\phi$ | 1 | 2 | −1/2 | (0, −1) | −1 | +1 | 0 |

processes. The model therefore has high potential for discovery by a variety of complementary experimental searches.

## 2. Model and low-energy effective theory

We introduce a Majorana fermionic DM particle $S$, a vectorlike heavy quark $\Psi$ that carries SM color and hypercharge, and a scalar $\phi$ that is an inert $SU(2)_L$ doublet. The quantum numbers are shown in Table 1. The only couplings of the new fields to SM particles allowed by gauge and global symmetries (see Table 1) are

$$-\mathcal{L} \ni \tilde{\lambda}_i \bar{Q}_{i,a}\phi^a \Psi + \lambda_i \bar{S}\phi_a^* L_i^a + \text{H.c.} + \lambda_{H,1}|H|^2|\phi|^2 + \lambda_{H,2}|H^\dagger\phi|^2 \quad (2)$$

where $Q, L$ are the SM quark and lepton doublets, $a$ is the $SU(2)_L$ index and $i$ is the flavor index. The relevant interactions at low energy are generated at one loop and thus require sizable couplings. Since there is no flavor symmetry, we will see that this model lives in a corner of parameter space where meson mixing constraints are nearly saturated. In a more complete model, the global symmetries could be an accidental consequence of a spontaneously broken gauge symmetry under which the new physics particles are charged.

The Higgs portal couplings $\lambda_{H,i}$ play no important role in the following; $\lambda_{H,1}$ gives an overall shift to $m_\phi^2$ after electroweak symmetry breaking, while $\lambda_{H,2}$ splits the charged and neutral components of $\phi$ by a small amount (relative to $m_\phi^2$ as constrained by LHC searches). A coupling of the form

$$\lambda_{H,3}(H^\dagger\phi)^2 + \text{H.c.} \quad (3)$$

violates lepton number conservation, as can be seen from the charge assignments in Table 1. (Notice that $S$ cannot be assigned lepton number since it is Majorana.) Of course one expects that $L$ is only an approximate symmetry, if neutrinos have Majorana masses, which constrains the size of $\lambda_{H,3}$. In fact this operator could be the origin of one of the neutrino masses through the loop diagram shown in Fig. 2, with mass matrix $\delta m_{\nu,ij} \sim \lambda_i\lambda_j\lambda_{H,3}m_S v^2/(16\pi^2 m_\phi^2)$ (where $v = 246$ GeV), which has a single nonvanishing eigenvalue given by the trace.[2] If $m_{\nu,3} = 0.05$ eV for example, $\lambda_{H,3} \sim 10^{-9}/\sum_i \lambda_i^2$.

To make definite predictions from (2), we must specify which field bases are referred to. We will assume that for the leptons and down-type quarks, it is the mass eigenbasis. This implies that up-type quarks have couplings that are rotated by the CKM matrix:

$$\tilde{\lambda}_i \bar{Q}_i \to \tilde{\lambda}_j \left( \bar{u}_{L,i} V_{ij}, \quad \bar{d}_{L,j} \right) \equiv \left( \tilde{\lambda}'_i \bar{u}_i, \tilde{\lambda}_i \bar{d}_i \right) \quad (4)$$

The box diagrams relevant for $b \to s\ell^+\ell^-$, $\ell_i \to 3\ell_j$, neutral meson mixing and DM scattering on nucleons are shown in Fig. 1.[3]

[2] A more complicated model with two or more flavors of dark matter would allow for nonsingular mass matrices.

[3] The $SU(2)_L$ charges of the fields in this theory do not allow it to contribute to $b \to s\nu\bar{\nu}$ at one loop.

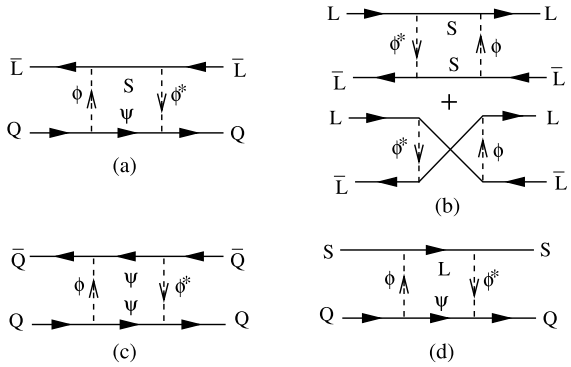


**Fig. 1.** Diagrams leading to (a) $b \to s\mu\mu$, (b) $\tau \to 3\mu$, (c) $B_s$–$\bar{B}_s$ mixing and (d) dark matter scattering on quarks. Arrows on the $\phi$ scalars show the flow of $SU(2)_L$ quantum number, presumed to not be carried by $S$ or $\Psi$.

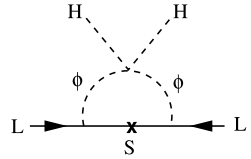


**Fig. 2.** Loop-induced contribution to light neutrino Majorana mass.

**Table 2**
Effective Hamiltonian dimension 6 operators and coefficients; $(\bar{f}_1 f_2)(\bar{f}_3 f_4)$ denotes $(\bar{f}_{1L}\gamma^\mu f_{2L})(\bar{f}_{3L}\gamma_\mu f_{4L})$ (with the exception of $(\bar{S}S)$, which corresponds to $\frac{1}{2}(\bar{S}\gamma_\mu\gamma_5 S)$) and coefficients are in units of $1/(384\pi^2 M^2)$ with $m_\Psi = m_\phi = M$ and loop functions $f_i$ given in text. $r \equiv m_S^2/M^2$.

| operator | coefficient | operator | coefficient |
|---|---|---|---|
| $(\bar{s}b)(\bar{\mu}\mu)$ | $2\tilde{\lambda}_2\tilde{\lambda}_3^*\lambda_2\|^2 f_1(r)$ | $(\bar{\mu}\mu)(\bar{\mu}\tau)$ | $4\lambda_2^*\|\lambda_2\|^2\lambda_3 f_2(r)$ |
| $(\bar{s}b)(\bar{s}b)$ | $\tilde{\lambda}_2^2\tilde{\lambda}_3^{*2}$ | $(\bar{d}d[\bar{u}u])(\bar{S}S)$ | $2\|\lambda_2\|^2\|\tilde{\lambda}_1^{[\prime]}\|^2 f_1(0)$ |

Evaluating them we find the effective dimension-6 operators of the same form as (1) but different external states. The operator coefficients are shown in Table 2, where for simplicity we take $m_\Psi = m_\phi = M$. Below we will see that $M \gtrsim 1$ TeV to meet LHC constraints, but $S$ can be light since it is dark matter. The loop functions $f_{1,2}$ are given by $f_1(r) = (3/2)(3r^2 - 2r^2\ln(r) - 4r + 1)/(1-r)^3$ and $f_2(r) = 3(-r^2 + 2r\ln(r) + 1)/(1-r)^3$, normalized such that $f_{1,2}(1) = 1$ and $f_1(0) = 3/2$ and $f_2(0) = 3$.

## 3. Flavor constraints

To match the observed $B$ anomalies, we require that $\tilde{\lambda}_2\tilde{\lambda}_3^*|\lambda_2|^2 \cong (M/0.88\ \text{TeV})^2$ [10]. Therefore the couplings must be of order unity, since LHC searches discussed below require $M \gtrsim 1$ TeV. On the other hand, strong $B_s$ mixing constraints, as determined by the mass splitting between $B_s$ and $\bar{B}_s$, limit the coefficient of $(\bar{s}b)^2$ in Table 2 to be less than $1/(408\ \text{TeV})^2$ at 95% confidence level (c.l.) [37], giving the bound $|\tilde{\lambda}_2\tilde{\lambda}_3| \lesssim M/(6.6\ \text{TeV})$. Combined with the previous determination, this demands large $\lambda_2$,

$$|\lambda_2| > 2.9\ (M/\text{TeV})^{1/2}\ . \quad (5)$$

Analogous bounds arise from $K$, $D$ and $B_d$ [50,51] mixing: $|\tilde{\lambda}_1\tilde{\lambda}_2| \lesssim M/(345\ \text{TeV})$, $|\tilde{\lambda}'_1\tilde{\lambda}'_2| \lesssim M/(110\ \text{TeV})$. $|\tilde{\lambda}_1\tilde{\lambda}_3| \lesssim M/(17\ \text{TeV})$.

As an example, suppose that $M = 1$ TeV and the bound on $B_s$ mixing is saturated. We can satisfy all other constraints with hierarchical quark couplings

$$|\tilde{\lambda}_1| = 0.014, \quad |\tilde{\lambda}_2| = 0.14, \quad |\tilde{\lambda}_3| = 1.1, \quad |\lambda_2| = 2.9 \quad (6)$$

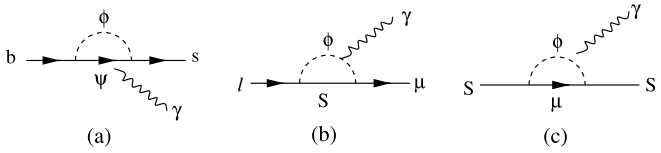


**Fig. 3.** Diagrams leading to (a) $b \to s\gamma$, (b) $\tau \to \mu\gamma$, $\mu \to e\gamma$ or $(g-2)_\mu$, and (c) $S$ anapole moment.

If all of the couplings are positive and real, $\tilde{\lambda}'_1\tilde{\lambda}'_2 = 0.009$, right at the $D$ mixing 95% c.l. limit. If $\tilde{\lambda}_1$ has the opposite sign to $\tilde{\lambda}_{2,3}$, $\tilde{\lambda}'_1\tilde{\lambda}'_2$ is smaller, $\cong 0.004$.

The hierarchical nature of the quark couplings is preserved under renormalization group running, since they are multiplicatively renormalized. The one-loop beta functions take the form [52,53]

$$\beta(\tilde{\lambda}_i) \equiv \mu\frac{d}{d\mu}\tilde{\lambda}_i = \frac{3}{16\pi^2}\,\tilde{\lambda}_i\left(\tfrac{1}{2}|\tilde{\lambda}_i|^2 + \sum_k |\tilde{\lambda}_k^2|\right) \tag{7}$$

For the choice of couplings in (6), this leads to a Landau pole in $\tilde{\lambda}_2$ at a scale of around $8m_\phi$, indicating the need for further new physics at such scales. For example a spontaneously broken non-abelian gauge symmetry, such as we already suggested for explaining the global symmetries of the model, could avert the Landau pole.

It is technically natural to assume the other leptonic couplings $\lambda_{1,3}$ are negligible, since they are generated radiatively only through neutrino mass insertions. However aesthetically it may seem peculiar to have $\lambda_2 \gg \lambda_3$. If $\lambda_{1,3} \neq 0$, the box diagrams leads to lepton flavor-violating decays such as $\tau \to 3\mu$ and $\mu \to 3e$. However because of the Majorana nature of $S$, there are crossed box diagrams, shown in Fig. 1, that exactly cancel the uncrossed ones in the limit where external momenta are neglected in the loop. Their amplitudes then scale as $\lambda_3\lambda_2^3 m_\tau^2/m_\phi^4$ and $\lambda_2\lambda_1^3 m_\mu^2/m_\phi^4$ respectively. After comparing them to those of leptonic decays in the SM, $2\sqrt{2}\,G_F(\bar{\nu}_i\gamma^\mu\ell_i)(\bar{\ell}_j\gamma^\mu\nu_j)$, and imposing the experimental limits on the forbidden decay modes [54] we find no significant constraints on $\lambda_1$ or $\lambda_3$.

Radiative transitions are another flavor-sensitive observable, as shown in Fig. 3. For $b \to s\gamma$, Fig. 3(a) generates the dipole operator

$$\frac{\tilde{\lambda}_3^*\tilde{\lambda}_2 e m_b}{32\pi^2}\left(q_\psi\frac{f(R)}{m_\phi^2} - q_\phi\frac{f(R^{-1})}{m_\psi^2}\right)(\bar{s}_L q\gamma^\mu b_R) \tag{8}$$

where $f(R) = (R^3 - 6R^2 + 3R + 6R\ln R + 2)/(6(R-1)^4)$, $R = m_\Psi^2/m_\phi^2$, $q$ is the photon momentum and $f(1) = 1/12$. The electric charges $q_i$ of $\Psi$ and $\phi$ are as in Table 1. Due to operator mixing, the chromomagnetic moment also contributes. Using the results of ref. [37], the Wilson coefficients for our benchmark model with $m_\phi = m_\Psi = 1$ TeV give $C_7 + 0.24\,C_8 = -9\times10^{-3}$, a factor of 10 below the current limit on this combination from measurements of the branching ratio of $b \to s\gamma$.

Fig. 3(b) gives a contribution to the anomalous magnetic moment of the muon of $\Delta(g-2)/2 \cong -(\lambda_2 m_\mu/\sqrt{96}\pi m_\phi)^2 \cong -1\times10^{-10}$, by saturating (5) and taking $m_\phi = 1$ TeV. Ultimately this model increases the tension between the measured and predicted values of $g-2$, but the effect is minimal, 20 times smaller than the SM discrepancy [54]. A similar diagram with the photon replaced by the $Z$ leads to a correction of the coupling of the $Z$ to left-handed muons of the form $\delta g_L/g_L^{\rm SM}(q^2 = m_Z^2) \cong -(\lambda_2 m_Z/24\pi m_\phi)^2 \cong -0.0012\%$ [37]. This is significantly smaller than the uncertainty on the most accurate measurements of this coupling by LEP, $g_L(m_Z^2) = -0.2689 \pm 0.0011$ [55], which has a 0.4% error at the $1\sigma$ level.

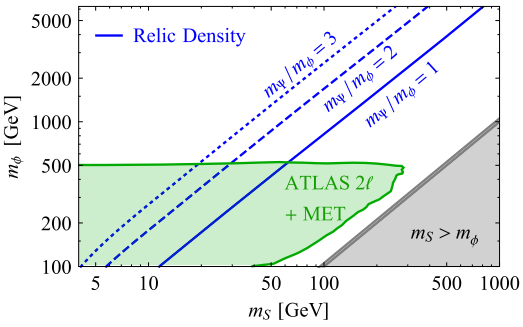


**Fig. 4.** Excluded regions in the plane of $m_\phi$ versus $m_S$ from an ATLAS slepton search [57] (green), and the requirement that $S$ is the lightest particle so that it can be the DM (grey). The blue lines correspond to values of $m_\phi$ and $m_S$ that give the correct relic density for different values of the ratio $m_\Psi/m_\phi$. $\lambda_2$ is set everywhere to the minimum value that allows for explanation of the flavor anomalies while avoiding $B_s$ mixing constraints. (For interpretation of the colors in the figure(s), the reader is referred to the web version of this article.)

If the couplings $\lambda_1$, $\lambda_3$ are nonzero, there are contributions to $\tau \to \mu\gamma$, $\tau \to e\gamma$, and $\mu \to e\gamma$, with partial width $\delta\Gamma \cong \mu_{i,j}^2 m_i^3/8\pi$ [56] where $\mu_{i,j} \cong e\lambda_i\lambda_j m_i/192\pi^2 m_\phi^2$. Using $\lambda_2 = 2.9$ and $m_\phi = 1$ TeV, the requirement that the partial width of $\tau \to \mu\gamma$ induced by the new physics contributions not exceed the measured value requires $|\lambda_3| < 0.8$, while $\mu \to e\gamma$ leads to the strong limit $|\lambda_1| < 1\times10^{-3}$.

## 4. Dark matter constraints

The dark matter candidate in our model has tree-level annihilation to $\mu\bar{\mu}$ and $\nu_\mu\bar{\nu}_\mu$. The $s$-wave contribution to the cross section is helicity suppressed, so the $v^2$ term dominates [61]. The total thermally averaged annihilation cross section, counting both final states, either muons or neutrinos, is

$$\langle\sigma\, v_{\rm rel}\rangle(x) = \frac{|\lambda_2|^4 m_S^2(m_\phi^4 + m_S^4)}{4\pi\,(m_\phi^2 + m_S^2)^4 x} \tag{9}$$

where $x = m_S/T$. To get the observed relic density [62], at the freeze-out temperature $T_f$ this should be roughly equal to the standard value $\langle\sigma\, v_{\rm rel}\rangle_0 \cong 4.6\times10^{-26}$ cm$^3$/s [63] appropriate for $p$-wave annihilating Majorana dark matter in the mass range $m_S \gtrsim 50$ GeV, that we will see is required by collider constraints. By assuming that $\lambda_2$ saturates the inequality (5) so that it is no larger than needed to satisfy the flavor constraints, the relation $\sigma\, v_{\rm rel}(x_f) = \langle\sigma\, v_{\rm rel}\rangle_0$ requires

$$m_S = 0.026\sqrt{x_f}\,m_\phi\,. \tag{10}$$

This is valid if $m_\phi \geq m_\Psi$; one can show that (10) is further reduced by the factor $m_\phi/m_\Psi$ if $m_\phi < m_\Psi$.

We verified the previous estimate by numerically solving the Boltzmann equation with micrOMEGAs 4.3.5 [64]; contours corresponding to the cosmologically preferred value $\Omega h^2 = 0.1199$ [62] are displayed in Fig. 4. $S$ annihilations can lead to indirect signals in gamma rays and charged cosmic rays, but the $p$-wave suppression of the cross section makes the limits from such searches very weak. Collider limits are far more constraining, notably ATLAS searches for 2 leptons and missing transverse energy [57], which exclude the green region in Fig. 4.

Because $S$ is a Majorana particle, the box diagram for scattering of $S$ off quarks leads only to spin-dependent or velocity-suppressed scattering off nucleons. The spin-dependent cross section for DM scattering off a single nucleon is given by $\sigma = \sigma_0\left(|\tilde{\lambda}_1|^2\Delta_d^{(n)} + |\tilde{\lambda}'_1|^2\Delta_u^{(n)} + |\tilde{\lambda}_2|^2\Delta_s^{(n)}\right)^2$, where $\sigma_0 = 3\mu_{n,S}^2|\lambda_2|^4/$

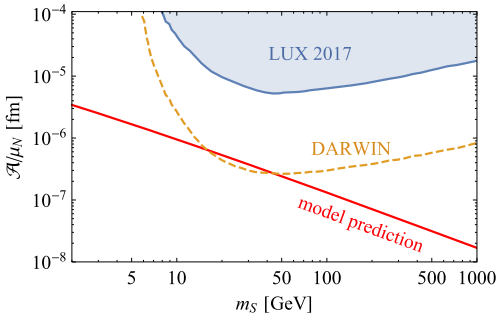


**Fig. 5.** The current limit on the anapole moment from LUX at 90% c.l. [58,59] and the estimated eventual sensitivity of the DARWIN experiment [60]. The prediction of our model for this quantity, based on the need to achieve the correct relic density and explain the $B$ anomalies, is shown by the red curve.

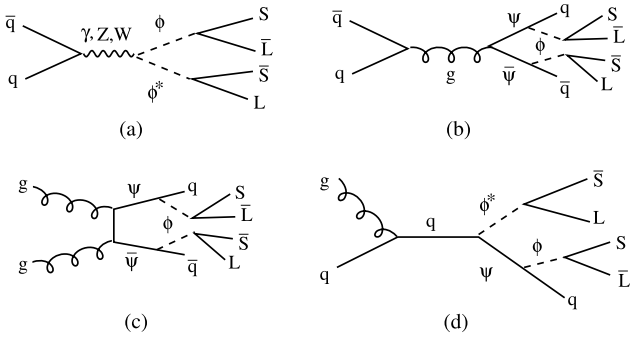


**Fig. 6.** Processes for production of quark jets, leptons, and missing energy.

$(256\pi^{5/2}M^2)^2$ for low-energy scattering (e.g. [65]). The determination of the $\Delta_q^{(n)}$ parameters is reviewed in [66]. For our benchmark model with $M = 1$ TeV this leads to $\sigma \sim 10^{-50}$ cm$^2$ for scattering off neutrons, far below current experimental limits on spin-dependent scattering from the PICO-60 direct detection experiment [67].

Had the dark matter been Dirac, diagram (c) of Fig. 3 would give both a magnetic moment for the dark matter $\mu_S \cong e|\lambda_2|^2 m_S/(64\pi^2 m_\phi^2)$, [approximating $m_S \ll m_\phi$ consistently with eq. (10)], and a charge-radius interaction $(\bar{S}\gamma_\mu S)\partial_\nu F^{\mu\nu}$ that lead to scattering on protons. Although the former is below current direct detection limits, the latter is far too large, which obliges us to take $S$ to be Majorana.[4] Then there is only an anapole moment $\mathcal{A}(\bar{S}\gamma_\mu\gamma_5 S)\,\partial_\nu F^{\mu\nu}$, which has been computed and constrained (using 2013 LUX results) for our class of models in ref. [58]. We rescale their limit on $\mathcal{A}$ to reflect more recent results from LUX [59], as well as the projected eventual sensitivity of DARWIN [60], in Fig. 5. The predicted value is also shown, using (5) and (10) with $x_f = 22$ to eliminate $\lambda_2$ and $m_\phi$ in favor of $m_S$. For the lowest allowed value of $m_S = 60$ GeV (considering that $m_\phi \gtrsim 500$ GeV from LHC constraints), the limit is a factor of 22.5 weaker than the prediction, corresponding to a factor of 500 in the cross section. This is below the reach of the LZ experiment [68], but slightly above the expected sensitivity of DARWIN, leaving open the possibility of direct detection.

## 5. Collider constraints

The new states $\phi$ and $\Psi$ carry SM quantum numbers, and can therefore be pair-produced in particle collisions. Fig. 6 shows the main production modes at a hadron collider and their decays. The final states necessarily include hard lepton pairs, since the splitting between $m_\phi$ and $m_S$ must be large, eq. (10). This also produces missing energy as the decay products inevitably include dark matter $S\bar{S}$ pairs. Moreover hadronic jets appear if $\Psi$ is produced, since $\Psi$ decays into $\phi$ plus quarks.

For Drell–Yan production of $\phi$–$\phi^*$ pairs, the signal is lepton pairs and missing energy, with no jets. (One of the leptons is a neutrino if $q\bar{q} \to W \to \phi^\pm\phi^0$ occurs.) This is the same final state as in production of slepton pairs, so SUSY searches [57] may be applied.[5] The excluded region is shown in Fig. 4, constraining $m_\phi \gtrsim 500$ GeV for all $m_S$ for which the relic density can be accommodated.

In diagrams (Fig. 6(b, c, d)), $\Psi$ is produced, which subsequently decays to $b\mu^+ S$ or $t\bar{\nu}_\mu S$. Such final states have been searched for by ATLAS in 13.3 fb$^{-1}$ of $\sqrt{s} = 13$ TeV data, including events with one or two leptons, jets and missing transverse momentum [69,70]. These analyses has been implemented in CheckMATE 2.0.14 [72], which we used to constrain our model, in conjunction with FeynRules 2.3 [73] and MadGraph 2.6.0 [71]. 20,000 events per model point were generated for the process $pp \to \Psi\bar{\Psi}$ ($pp \to \Psi\phi^*$ is suppressed by the small couplings of $\Psi$ and $\phi$ to first generation quarks, or the parton distribution function of $b$ or $t$). The subsequent showering and hadronization of the final state partons was modeled with Pythia 8.230 [74] and detector simulation was done with Delphes 3.4.1 [75].

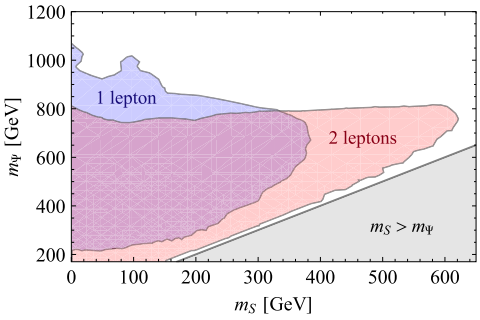


**Fig. 7.** Shaded regions in the $m_S$–$m_\Psi$ plane are excluded at 95% c.l. by ATLAS run 2 searches for one (blue) or two (red) leptons, jets, and missing energy [69,70]. For each point, $m_S$ and the couplings are set as described in text to satisfy flavor and DM relic density constraints.

Fig. 7 shows the resulting 95% c.l. limits on $m_\Psi$ versus $m_S$ for models which both explain the flavor anomalies and give the correct DM relic density. Here $m_\phi$ is set by eq. 10 with $x_f = 22$ and the couplings are scaled relative to (6) by the factor $(M/1\text{ TeV})^{1/2}$, where $M = \max(m_\phi, m_\Psi)$; this choice keeps all the box diagrams approximately constant. At values of $m_S \lesssim 60$ GeV, the lowest values that allow for the correct relic density while avoiding slepton search constraints, the one-lepton search limits $m_\Psi \gtrsim 950$ GeV, except for a narrow window with $m_S$ just below $m_\phi$. The two-lepton search does not constrain $m_\Psi$ as strongly but is more sensitive to larger DM masses.

## 6. Conclusions

The indications from LHCb of lepton flavor universality breaking down are currently our best hint of physics beyond the standard

[4] We thank S. Okawa for pointing out the importance of the charge radius contribution.

[5] These limits assume annihilation to all flavors of both right and left handed sleptons, taken to be degenerate. Comparing production cross sections of all sleptons to that of a $\phi\phi^*$ pair using MadGraph [71] indicates that they may be overly stringent for our model; at 13 TeV, the slepton production cross section is $\sigma = 1.40$ fb for $m_{\tilde{\ell}} = 500$ GeV, whereas $\sigma = 0.33$ fb for $\phi\phi^*$ production with $m_\phi = 500$ GeV.

model from colliders. These anomalies should be verified within a few years by further data from LHCb and Belle II [76]. If confirmed, it is not unreasonable to expect that the relevant new physics could also shed light on other shortcomings of the standard model. We have shown how a very economical model, in which dark matter plays an essential role, could be the source of $R(K^{(*)})$ anomalies, while predicting imminent tensions in other flavor observables, notably $B_s$ mixing. The model may be tested by the next generation of direct detection searches and can be discovered at the LHC via searches for leptons, jets and missing energy.

## Acknowledgements

We thank J. Martin Camalich and D. London for helpful discussions, and S. Okawa for alerting us to a problem with the first version of this paper. Our work is supported by the Natural Sciences and Engineering Research Council (NSERC) of Canada.

## References

[1] Roel Aaij, et al., LHCb, Test of lepton universality using $B^+ \to K^+\ell^+\ell^-$ decays, Phys. Rev. Lett. 113 (2014) 151601, arXiv:1406.6482 [hep-ex].
[2] R. Aaij, et al., LHCb, Test of lepton universality with $B^0 \to K^{*0}\ell^+\ell^-$ decays, J. High Energy Phys. 08 (2017) 055, arXiv:1705.05802 [hep-ex].
[3] Gudrun Hiller, Frank Kruger, More model-independent analysis of $b \to s$ processes, Phys. Rev. D 69 (2004) 074020, arXiv:hep-ph/0310219.
[4] Marzia Bordone, Gino Isidori, Andrea Pattori, On the Standard Model predictions for $R_K$ and $R_{K^*}$, Eur. Phys. J. C 76 (2016) 440, arXiv:1605.07633 [hep-ph].
[5] Bernat Capdevila, Andreas Crivellin, Sébastien Descotes-Genon, Joaquim Matias, Javier Virto, Patterns of New Physics in $b \to s\ell^+\ell^-$ transitions in the light of recent data, arXiv:1704.05340 [hep-ph], 2017.
[6] Li-Sheng Geng, Benjamín Grinstein, Sebastian Jäger, Jorge Martin Camalich, Xiu-Lei Ren, Rui-Xiang Shi, Towards the discovery of new physics with lepton-universality ratios of $b \to s\ell\ell$ decays, Phys. Rev. D 96 (2017) 093006, arXiv:1704.05446 [hep-ph].
[7] Marco Ciuchini, Antonio M. Coutinho, Marco Fedele, Enrico Franco, Ayan Paul, Luca Silvestrini, Mauro Valli, On Flavourful Easter eggs for New Physics hunger and Lepton Flavour Universality violation, Eur. Phys. J. C 77 (2017) 688, arXiv:1704.05447 [hep-ph].
[8] Gudrun Hiller, Ivan Nisandzic, $R_K$ and $R_{K^*}$ beyond the standard model, Phys. Rev. D 96 (2017) 035003, arXiv:1704.05444 [hep-ph].
[9] Wolfgang Altmannshofer, Peter Stangl, David M. Straub, Interpreting hints for lepton flavor universality violation, Phys. Rev. D 96 (2017) 055008, arXiv:1704.05435 [hep-ph].
[10] Guido D'Amico, Marco Nardecchia, Paolo Panci, Francesco Sannino, Alessandro Strumia, Riccardo Torre, Alfredo Urbano, Flavour anomalies after the $R_{K^*}$ measurement, J. High Energy Phys. 09 (2017) 010, arXiv:1704.05438 [hep-ph].
[11] Stefano Di Chiara, Andrew Fowlie, Sean Fraser, Carlo Marzo, Luca Marzola, Martti Raidal, Christian Spethmann, Minimal flavor-changing $Z'$ models and muon $g-2$ after the $R_{K^*}$ measurement, Nucl. Phys. B 923 (2017) 245–257, arXiv:1704.06200 [hep-ph].
[12] Cheng-Wei Chiang, Xiao-Gang He, Jusak Tandean, Xing-Bo Yuan, $R_{K^{(*)}}$ and related $b \to s\ell\bar{\ell}$ anomalies in minimal flavor violation framework with $Z'$ boson, Phys. Rev. D 96 (2017) 115022, arXiv:1706.02696 [hep-ph].
[13] Mykhailo Dalchenko, Bhaskar Dutta, Ricardo Eusebi, Peisi Huang, Teruki Kamon, Denis Rathjens, Bottom-quark fusion processes at the LHC for probing $Z'$ models and B-meson decay anomalies, arXiv:1707.07016 [hep-ph], 2017.
[14] Pankaj Agrawal, Debashis Saha, Ambresh Shivaji, Production of $HHH$ and $HHV(V=\gamma,Z)$ at the hadron colliders, Phys. Rev. D 97 (2018) 036006, arXiv:1708.03580 [hep-ph].
[15] Miguel Crispim Romao, Stephen F. King, George K. Leontaris, Non-universal $Z'$ from fluxed GUTs, arXiv:1710.02349 [hep-ph], 2017.
[16] Faisel Gaber, Jusak Tandean, Connecting $b \to s\ell\bar{\ell}$ anomalies to enhanced rare nonleptonic $\bar{B}_s^0$ decays in $Z'$ model, J. High Energy Phys. 02 (2018) 074, arXiv:1710.11102 [hep-ph].
[17] Adam Falkowski, Stephen F. King, Elena Perdomo, Mathias Pierre, Flavourful $Z'$ portal for vector-like neutrino Dark Matter and $R_{K^{(*)}}$, arXiv:1803.04430 [hep-ph], 2018.
[18] Masaya Kohda, Tanmoy Modak, Abner Soffer, Identifying a $Z'$ behind $b \to s\ell\ell$ anomalies at the LHC, arXiv:1803.07492 [hep-ph], 2018.
[19] Chuan-Hung Chen, Takaaki Nomura, Hiroshi Okada, Excesses of muon $g-2$, $R_{D^{(*)}}$, and $R_K$ in a leptoquark model, Phys. Lett. B 774 (2017) 456–464, arXiv:1703.03251 [hep-ph].
[20] Andreas Crivellin, Dario Müller, Toshihiko Ota, Simultaneous explanation of R(D*) and $b \to s\mu^+\mu^-$: the last scalar leptoquarks standing, J. High Energy Phys. 09 (2017) 040, arXiv:1703.09226 [hep-ph].
[21] Yi Cai, John Gargalionis, Michael A. Schmidt, Raymond R. Volkas, Reconsidering the one leptoquark solution: flavor anomalies and neutrino mass, J. High Energy Phys. 10 (2017) 047, arXiv:1704.05849 [hep-ph].
[22] Bhavesh Chauhan, Bharti Kindra, Ashish Narang, A leptoquark explanation for $(g-2)_\mu$, $R_K$, $R_{K^*}$ and, IceCube PeV events, arXiv:1706.04598 [hep-ph], 2017.
[23] Bastian Diaz, Martin Schmaltz, Yi-Ming Zhong, The leptoquark Hunter's guide: pair production, J. High Energy Phys. 10 (2017) 097, arXiv:1706.05033 [hep-ph].
[24] Ilja Doršner, Svjetlana Fajfer, Darius A. Faroughy, Nejc Košnik, The role of the $S_3$ GUT leptoquark in flavor universality and collider searches, J. High Energy Phys. 2017 (2017) 188, https://doi.org/10.1007/JHEP10(2017)188, arXiv:1706.07779 [hep-ph].
[25] Andreas Crivellin, Dario Müller, Adrian Signer, Yannick Ulrich, Correlating lepton flavor universality violation in $B$ decays with $\mu \to e\gamma$ using leptoquarks, Phys. Rev. D 97 (2018) 015019, arXiv:1706.08511 [hep-ph].
[26] Daniel Aloni, Avital Dery, Claudia Frugiuele, Yosef Nir, Testing minimal flavor violation in leptoquark models of the $R_{K^{(*)}}$ anomaly, J. High Energy Phys. 11 (2017) 109, arXiv:1708.06161 [hep-ph].
[27] Nima Assad, Bartosz Fornal, Benjamin Grinstein, Baryon number and lepton universality violation in leptoquark and diquark models, Phys. Lett. B 777 (2018) 324–331, arXiv:1708.06350 [hep-ph].
[28] Luca Di Luzio, Admir Greljo, Marco Nardecchia, Gauge leptoquark as the origin of B-physics anomalies, Phys. Rev. D 96 (2017) 115011, arXiv:1708.08450 [hep-ph].
[29] Lorenzo Calibbi, Andreas Crivellin, Tianjun Li, A model of vector leptoquarks in view of the $B$-physics anomalies, arXiv:1709.00692 [hep-ph], 2017.
[30] Ujjal Kumar Dey, Deepak Kar, Manimala Mitra, Michael Spannowsky, Aaron C. Vincent, Searching for leptoquarks at IceCube and the LHC, arXiv:1709.02009 [hep-ph], 2017.
[31] Bhavesh Chauhan, Bharti Kindra, Invoking chiral vector leptoquark to explain LFU violation in B decays, arXiv:1709.09989 [hep-ph], 2017.
[32] Dario Müller, Leptoquarks in flavour physics, in: Workshop on Flavour Changing and Conserving Processes, FCCP2017, Anacapri, Capri Island, Italy, September 7–9, 2017, 2018, arXiv:1801.03380 [hep-ph].
[33] Ilja Doršner, Admir Greljo, Leptoquark toolbox for precision collider studies, arXiv:1801.07641 [hep-ph], 2018.
[34] Gudrun Hiller, Dennis Loose, Ivan Nišandžić, Flavorful leptoquarks at hadron colliders, Phys. Rev. D 97 (2018) 075004, arXiv:1801.09399 [hep-ph].
[35] S. Fajfer, N. Košnik, L. Vale Silva, Footprints of leptoquarks: from $R_{K^{(*)}}$ to $K \to \pi\nu\bar{\nu}$, Eur. Phys. J. C 78 (2018) 275, arXiv:1802.00786 [hep-ph].
[36] Angelo Monteux, Arvind Rajaraman, B anomalies and leptoquarks at the LHC: beyond the lepton-quark final state, arXiv:1803.05962 [hep-ph], 2018.
[37] Pere Arnan, Lars Hofer, Federico Mescia, Andreas Crivellin, Loop effects of heavy new scalars and fermions in $b \to s\mu^+\mu^-$, J. High Energy Phys. 04 (2017) 043, arXiv:1608.07832 [hep-ph].
[38] Ben Gripaios, M. Nardecchia, S.A. Renner, Linear flavour violation and anomalies in B physics, J. High Energy Phys. 06 (2016) 083, arXiv:1509.05020 [hep-ph].
[39] D. Aristizabal Sierra, Florian Staub, Avelino Vicente, Shedding light on the $b \to s$ anomalies with a dark sector, Phys. Rev. D 92 (2015) 015001, arXiv:1503.06077 [hep-ph].
[40] Geneviève Bélanger, Cédric Delaunay, Susanne Westhoff, A dark matter relic from muon anomalies, Phys. Rev. D 92 (2015) 055021, arXiv:1507.06660 [hep-ph].
[41] Alejandro Celis, Wan-Zhe Feng, Martin Vollmann, Dirac dark matter and $b \to s\ell^+\ell^-$ with U(1) gauge symmetry, Phys. Rev. D 95 (2017) 035018, arXiv:1608.03894 [hep-ph].
[42] Wolfgang Altmannshofer, Stefania Gori, Stefano Profumo, Farinaldo S. Queiroz, Explaining dark matter and B decay anomalies with an $L_\mu - L_\tau$ model, J. High Energy Phys. 12 (2016) 106, arXiv:1609.04026 [hep-ph].
[43] James M. Cline, Jonathan M. Cornell, David London, Ryoutaro Watanabe, Hidden sector explanation of $B$-decay and cosmic ray anomalies, Phys. Rev. D 95 (2017) 095015, arXiv:1702.00395 [hep-ph].
[44] Seungwon Baek, Dark matter contribution to $b \to s\mu^+\mu^-$ anomaly in local $U(1)_{L_\mu - L_\tau}$ model, arXiv:1707.04573 [hep-ph], 2017.
[45] James M. Cline, $B$ decay anomalies and dark matter from vectorlike confinement, arXiv:1710.02140 [hep-ph], 2017.
[46] Filippo Sala, David M. Straub, A new light particle in B decays?, Phys. Lett. B 774 (2017) 205–209, arXiv:1704.06188 [hep-ph].
[47] Junichiro Kawamura, Shohei Okawa, Yuji Omura, Interplay between the b $\to s\ell\ell$ anomalies and dark matter physics, Phys. Rev. D 96 (2017) 075041, arXiv:1706.04344 [hep-ph].
[48] Cheng-Wei Chiang, Guan-Jie Huang, Hiroshi Okada, A simple model for explaining muon-related anomalies and dark matter, arXiv:1711.07365 [hep-ph], 2017.
[49] Bhubanjyoti Bhattacharya, David London, James M. Cline, Alakabha Datta, Grace Dupuis, Quark-flavored scalar dark matter, Phys. Rev. D 92 (2015) 115012, arXiv:1509.04271 [hep-ph].
[50] M. Bona, et al., UTfit, Model-independent constraints on $\Delta F = 2$ operators and the scale of new physics, J. High Energy Phys. 03 (2008) 049, arXiv:0707.0636 [hep-ph].

[51] Marcella Bona, UTfit, Unitarity triangle analysis beyond the Standard Model from UTfit, Proceedings, 38th International Conference on High Energy Physics (ICHEP 2016): Chicago, IL, USA, August 3–10, 2016, PoS ICHEP2016 (2016) 149.
[52] Ming-xing Luo, Yong Xiao, Two loop renormalization group equations in the standard model, Phys. Rev. Lett. 90 (2003) 011601, arXiv:hep-ph/0207271.
[53] Marie E. Machacek, Michael T. Vaughn, Two loop renormalization group equations in a general quantum field theory. 1. Wave function renormalization, Nucl. Phys. B 222 (1983) 83–103.
[54] C. Patrignani, et al., Particle Data Group, Review of particle physics, Chin. Phys. C 40 (2016) 100001.
[55] S. Schael, et al., SLD Electroweak Group, DELPHI, ALEPH, SLD, SLD Heavy Flavour Group, OPAL, LEP Electroweak Working Group, L3, Precision electroweak measurements on the $Z$ resonance, Phys. Rep. 427 (2006) 257–454, arXiv:hep-ex/0509008.
[56] Carlo Giunti, Alexander Studenikin, Neutrino electromagnetic interactions: a window to new physics, Rev. Mod. Phys. 87 (2015) 531, arXiv:1403.6344 [hep-ph].
[57] The ATLAS collaboration (ATLAS), Search for electroweak production of supersymmetric particles in the two and three lepton final state at $\sqrt{s} = 13$ TeV with the ATLAS detector, ATLAS-CONF-2017-039 (2017).
[58] Joachim Kopp, Lisa Michaels, Juri Smirnov, Loopy constraints on leptophilic dark matter and internal bremsstrahlung, J. Cosmol. Astropart. Phys. 1404 (2014) 022, arXiv:1401.6457 [hep-ph].
[59] D.S. Akerib, et al., LUX, Results from a search for dark matter in the complete LUX exposure, Phys. Rev. Lett. 118 (2017) 021303, arXiv:1608.07648 [astro-ph.CO].
[60] J. Aalbers, et al., DARWIN, DARWIN: towards the ultimate dark matter detector, J. Cosmol. Astropart. Phys. 1611 (2016) 017, arXiv:1606.07001 [astro-ph.IM].
[61] Spencer Chang, Ralph Edezhath, Jeffrey Hutchinson, Markus Luty, Leptophilic effective WIMPs, Phys. Rev. D 90 (2014) 015011, arXiv:1402.7358 [hep-ph].
[62] P.A.R. Ade, et al., Planck, Planck 2015 results. XIII. Cosmological parameters, Astron. Astrophys. 594 (2016) A13, arXiv:1502.01589 [astro-ph.CO].
[63] Gary Steigman, Basudeb Dasgupta, John F. Beacom, Precise relic WIMP abundance and its impact on searches for dark matter annihilation, Phys. Rev. D 86 (2012) 023506, arXiv:1204.3622 [hep-ph].
[64] G. Belanger, F. Boudjema, A. Pukhov, A. Semenov, MicrOMEGAs 2.0: a program to calculate the relic density of dark matter in a generic model, Comput. Phys. Commun. 176 (2007) 367–382, arXiv:hep-ph/0607059.
[65] G. Belanger, F. Boudjema, A. Pukhov, A. Semenov, Dark matter direct detection rate in a generic model with micrOMEGAs 2.2, Comput. Phys. Commun. 180 (2009) 747–767, arXiv:0803.2360 [hep-ph].
[66] Torsten Bringmann, et al., DarkBit: a GAMBIT module for computing dark matter observables and likelihoods, Eur. Phys. J. C 77 (2017) 831, arXiv:1705.07920 [hep-ph].
[67] C. Amole, et al., PICO, Dark matter search results from the PICO-60 $C_3F_8$ bubble chamber, Phys. Rev. Lett. 118 (2017) 251301, arXiv:1702.07666 [astro-ph.CO].
[68] M. Szydagis, LUX, LZ, The present and future of searching for dark matter with LUX and LZ, Proceedings, 38th International Conference on High Energy Physics, (ICHEP 2016): Chicago, IL, USA, August 3–10, 2016, PoS ICHEP2016 (2016) 220, arXiv:1611.05525 [astro-ph.CO].
[69] The ATLAS collaboration (ATLAS), Search for top squarks in final states with one isolated lepton, jets, and missing transverse momentum in $\sqrt{s} = 13$ TeV pp collisions with the ATLAS detector, ATLAS-CONF-2016-050 (2016).
[70] The ATLAS collaboration (ATLAS), Search for direct top squark pair production and dark matter production in final states with two leptons in $\sqrt{s} = 13$ TeV $pp$ collisions using 13.3 $\text{fb}^{-1}$ of ATLAS data, ATLAS-CONF-2016-076 (2016).
[71] J. Alwall, R. Frederix, S. Frixione, V. Hirschi, F. Maltoni, O. Mattelaer, H.S. Shao, T. Stelzer, P. Torrielli, M. Zaro, The automated computation of tree-level and next-to-leading order differential cross sections, and their matching to parton shower simulations, J. High Energy Phys. 07 (2014) 079, arXiv:1405.0301 [hep-ph].
[72] Manuel Drees, Herbi Dreiner, Daniel Schmeier, Jamie Tattersall, Jong Soo Kim, CheckMATE: confronting your favourite new physics model with LHC data, Comput. Phys. Commun. 187 (2015) 227–265, arXiv:1312.2591 [hep-ph].
[73] Adam Alloul, Neil D. Christensen, Céline Degrande, Claude Duhr, Benjamin Fuks, FeynRules 2.0 – a complete toolbox for tree-level phenomenology, Comput. Phys. Commun. 185 (2014) 2250–2300, arXiv:1310.1921 [hep-ph].
[74] Torbjörn Sjöstrand, Stefan Ask, Jesper R. Christiansen, Richard Corke, Nishita Desai, Philip Ilten, Stephen Mrenna, Stefan Prestel, Christine O. Rasmussen, Peter Z. Skands, An introduction to PYTHIA 8.2, Comput. Phys. Commun. 191 (2015) 159–177, arXiv:1410.3012 [hep-ph].
[75] J. de Favereau, C. Delaere, P. Demin, A. Giammanco, V. Lemaître, A. Mertens, M. Selvaggi, DELPHES 3, DELPHES 3, a modular framework for fast simulation of a generic collider experiment, J. High Energy Phys. 02 (2014) 057, arXiv:1307.6346 [hep-ex].
[76] Johannes Albrecht, Florian Bernlochner, Matthew Kenzie, Stefanie Reichert, David Straub, Alison Tully, Future prospects for exploring present day anomalies in flavour physics measurements with Belle II and LHCb, arXiv:1709.10308 [hep-ph], 2017.